Title

Targeting Galectin-1 Impairs Castration-Resistant Prostate Cancer Progression and Invasion

Journal

Clinical Cancer Research, 24(17)

ISSN

1078-0432

Authors

Shih, Tsung-Chieh

Liu, Ruiwu

Wu, Chun-Te

et al.

Publication Date

2018-09-01

DOI

10.1158/1078-0432.ccr-18-0157

Targeting Galectin-1 impairs castration-resistant prostate cancer progression and invasion

Authors:

Tsung-Chieh Shih[1], Ruiwu Liu[1]*, Chun-Te Wu[2], Xiaocen Li[1], Wenwu Xiao[1], Xiaojun Deng[1], Sophie Kiss[1], Ting Wang[3], Xiao-Jia Chen[4], Randy Carney[1], Hsing-Jien Kung[5], Yong Duan[3], Paramita M. Ghosh[1,6,7], Kit S. Lam[1,8]*

Affiliations:

[1] Department of Biochemistry and Molecular Medicine, University of California Davis, Sacramento, California, USA.

[2] Department of Urology, Chang Gung Memorial Hospital, Keelung, Taiwan

[3] Genome Center, University of California Davis, Davis, California, USA.

[4] Institute of Biomedicine & Cell Biology Department, Jinan University; National Engineering Research Center of Genetic Medicine; Guangdong Provincial Key Laboratory of Bioengineering Medicine; Guangdong Provincial Engineering Research Center of Biotechnological medicine, Guangdong, Guangzhou, China

[5] The Institute for Cancer Biology and Drug Discovery, Taipei Medical University, Taipei, Taiwan

[6] Department of Urology, School of Medicine, University of California Davis, Sacramento, California, USA.

[7] Veterans Affairs Northern California Health Care System–Mather, Mather, California, USA.

[8] Comprehensive Cancer Center, University of California Davis, Sacramento, California, USA.

Running title:

Targeting Galectin-1 impairs CRPC progression and invasion

Abbreviations list:

OB2C: one-bead two-compounds

mCRPC: metastatic castration resistant prostate cancer

PCa: prostate cancer

Gal-1: Galectin-1

SAR: structure-activity relationship

Corresponding authors:

Kit S. Lam (kslam@ucdavis.edu) and Ruiwu Liu (rwliu@ucdavis.edu). Department of Biochemistry & Molecular Medicine, University of California at Davis, Suite 2301, 2700 Stockton Blvd, Sacramento, CA 95817. Phone: 916-734-0910; FAX: 916-734-4418.

Conflict of interest:

Tsung-Chieh Shih, Ruiwu Liu and Kit S. Lam are the inventors of LLS30.

Translational Relevance

The majority of PCa patients who are treated with androgen deprivation therapy (ADT) will eventually develop CRPC. Currently, patients with mCRPC are treated with the chemotherapeutic agent docetaxel, the inhibitors of the androgen receptor (AR) pathway – enzalutamide or abiraterone acetate, or Radium-223, but these treatments extend patient survival by only a few months each. Thus, there are no effective durable therapies for patients with CRPC. Both AR dependent and AR-independent signal pathways contribute to CRPC. Here, we report that Gal-1 expression was associated with advanced PCa, and that Gal-1 can control CRPC growth through both AR-dependent and AR-independent pathways. Our preclinical data demonstrate that Gal-1-targeting with LLS30 can effectively inhibit the CRPC growth and metastasis. The application of Gal-1-targeting deserves attention. This study provides the molecular rationale for the use of Gal-1 inhibitors, such as LLS30, in the treatment of AR-driven, as well as non-AR-driven, CRPC.

Abstract

Purpose: The majority of prostate cancer (PCa) patients who are treated with androgen deprivation therapy (ADT) will eventually develop fatal metastatic castration-resistant prostate cancer (mCRPC). Currently, there are no effective durable therapies for patients with mCRPC. High expression of Galectin-1 (Gal-1) is associated with PCa progression and poor clinical outcome. The role of Gal-1 in tumor progression are largely unknown. Here we characterized Gal-1 functions and evaluated the therapeutic effects of a newly developed Gal-1inhibitor, LLS30, in mCRPC.

Experimental Design: Cell viability, colony formation, migration and invasion assays were performed to examine the effects of inhibition of Gal-1 in CRPC cells. We used two human CRPC xenograft models to assess growth inhibitory effects of LLS30. Genome-wide gene expression analysis was conducted to elucidate the effects of LLS30 on metastatic PC3 cells.

Results: Gal-1 was highly expressed in CRPC cells, but not in androgen-sensitive cells. Gal-1 knockdown significantly inhibited CRPC cells' growth, anchorage independent growth, migration and invasion through the suppression of AR and Akt signaling. LLS30 targets Gal-1 as an allosteric inhibitor, and decreases Gal-1 binding affinity to its binding partners. LLS30 showed *in vivo* efficacy in both AR positive and AR negative xenograft models. LLS30 not only can potentiate the anti-tumor effect of docetaxel to cause complete regression of tumors, but can also effectively inhibit the invasion and metastasis of PCa cells *in vivo.*

Conclusions: Our study provides evidence that Gal-1 is an important target for mCRPC therapy, and LLS30 is a promising small molecule compound that can potentially overcome mCRPC.

Introduction

Prostate cancer (PCa) is the most common non-skin malignancy and the third leading cause of cancer death in men (1). While localized disease is treated with prostatectomy or radiation therapy, androgen deprivation therapy (ADT) is the initial treatment for patients with metastatic prostate cancer (2). Although ADT leads to remissions lasting ~2–3 years, most patients develop hormone independence and eventually form metastasis castration resistant prostate cancer (mCRPC). PCa mortality typically results from mCRPC, and median survival of men with mCRPC is 10 to 12 months (3). Currently, patients with mCRPC are treated with the chemotherapeutic agent docetaxel, the inhibitors of the androgen receptor (AR) pathway – enzalutamide or abiraterone acetate, the immunotherapy reagent Sipuleucel T or Radium-223, but these treatments extend patient survival by only a few months each.

Galectin-1 (Gal-1), a 14 kDa lectin, is a galectin family member with an affinity for β-galactosides. High expression of Gal-1 has been found in many human cancers including ovarian cancer (4), lung cancer (5), breast cancer (6), kidney cancer (7), pancreatic cancer (8). Gal-1 is associated with a variety of cellular processes, including cell proliferation (9), T cell apoptosis (10, 11), cell cycle (12, 13), angiogenesis (14), and metastatic spread of cancer (15-17). In PCa, Gal-1 is over-expressed in advanced and metastatic lesions, and elevated Gal-1 expression level correlates with worse outcome (18, 19). These clinical observations signify the importance of the role of Gal-1 in PCa. However, the molecular mechanisms underlying Gal-1-mediated tumor progression to date are largely unknown.

Given that increased expression of Gal-1 is associated with PCa progression and poor clinical outcome, Gal-1 is an excellent therapeutic target for treatment or prevention of mCRPC. LLS2, a novel Gal-1 inhibitor identified by the one-bead two-compound combinatorial technology, decreased membrane-associated Ras and disrupted downstream Erk pathway (20). LLS2 caused apoptosis in colon, pancreatic, ovarian, prostate and breast cancer cells, and showed *in vivo* efficacy in ovarian cancer xenografts. Since LLS2 is relatively less potent with a relatively high IC_{50} (15-35 μM in most cells tested), we further optimized LLS2 into a more potent Gal-1 inhibitor against mCRPC. Currently, there are few Gal-1 inhibitors that are universally effective and none have been developed for human use (21).

In this study, we focused on functional aspects of Gal-1 expression as it relate to clinical PCa tumor progression and metastasis. We also used LLS2 as scaffold to develop a novel Gal-1 selective inhibitor named LLS30. Gal-1 knockdown by siRNA significantly inhibited CRPC cell line proliferation, migration, invasion and anchorage-independent survival of AR positive and AR negative PCa cells.

Gal-1 can regulate prostate cancer independent of the AR pathway. Equally important, LLS30 showed *in vivo* efficacy in both AR positive and AR negative xenograft models without evidence of toxicity. Furthermore, LLS30 not only can potentiate the anti-tumor effect of docetaxel to cause complete regression of tumors, but can also effectively inhibit the invasion and metastasis of PCa cells *in vivo.*

Materials and methods

Synthesis of LLS30

LLS30 was synthesized on Fluoroenylmethyloxycarbonyl (Fmoc)-protected Rink-amide MBHA resin and was cleaved off the beads followed by purification with reversed-phase high-performance liquid chromatography (RP-HPLC). For detail of synthesis, please refer to Supplementary Materials and methods.

Patients samples

Prostate cancer tissue arrays of retropubic radical prostatectomy were obtained from University of California Davis Comprehensive Cancer Center (83 cases) and US Biomax (PR803b, 66 cases). The institutional ethics committee approved all of the protocols. Gleason grading was done on tissue core based on 2005 ISUP modified system(22): Gleason score<6 (low-grade or well differentiated), =7 (intermediate-grade or moderately differentiated), and >8 (high-grade or poorly differentiated). Human tissues covered 38 cases of benign hyperplasia (BHP), 32 cases of low-grade, 24 cases of intermediate -grade and 55 cases of high-grade PCa.

Cell lines

The sources of cell lines include AR positive 22RV1 and CWR-R1, and AR negative PC3 and DU145 prostate cancer cells. These cells were purchased from ATCC. Cells were maintained in RPMI1640 supplemented with 10% fetal bovine serum and 1% penicillin/streptomycin, and grown in 5% CO_2 at 37 ℃. Gal-1 was examined by Western blotting after transfection with siGal-1 and pcDNA/Gal-1. Morphology of PC3 cells was visualized by light microscopy after LLS30 treatment. Experiments were performed on cells with passage numbers below 20. Mycoplasma testing was routinely performed every month.

Cell proliferation assays

3 x 10^3 prostate cancer cells were seeded into 96-well plates. Cells were allowed to attach for 24 hr prior to drug treatment for 72 hr. After 24 hr, medium was removed and the cells were treated with the

indicated concentrations of LLS30 or siRNA. Cell viability was determined by CellTiter-Glo Luminescent Cell Viability Assay Kit after 72 hr.

Cell adhesion assay

Effect of LLS30 on adhesion of PC3 cells to collagen, fibronectin and laminin. The wells in 96-well plates were coated with collagen, fibronectin and laminin. PC3 cells were pre-treated with in RPMI1640 supplemented with 10% fetal bovine serum and 1% penicillin/streptomycin (control) or in presence of 5 μM LLS30 for 1 hour before plating into coated wells. After overnight culture, the number of adherent PC3 cells was quantified using CellTiter-Glo Luminescent Cell Viability Assay Kit.

Gene expression microarray

To explore the gene expression changes in PC3 cells treated with 10 μM LLS30 at multiple time points (0.5, 1, 2, 5, 24 hrs), we used HumanHT-12 v4 BeadChip (Illumina). The data normalization was done using GenomeStudio Software (Illumina). Genes that changed at least 1.5 fold and $p<0.05$ were selected for functional pathways analysis using KEGG & NCI database. The details for gene profiling, data analysis, are provided in Supplementary Materials and methods.

Establishment of Gal-1 knockdown Cells

CRPC were seeded on the 6 well plates. Cells were transfected with 50 nM negative control mimic or mixed siRNA against Gal-1 (Invitrogen, HSS106025 and Ambion, s194592) using Lipofectamine 2000 transfection reagent (Life Technologies) according to the manufacturer's instructions. CRPC cells were infected with control or Gal-1 shRNA lentiviral particles (Santa Cruz) at an MOI of 10 for 24 h in the presence of 8 μg/ml polybrene.

Colony formation Assays

500 CRPC cells with lentivirus carrying shRNA targeting control or Gal-1 were seeded into 24-well ultra-low attachment plates (Corning). The growth medium was replaced every 3 days. The colonies were formed after 10 days. Colonies were imaged for colony size calculation 5 days post treatment. Colony diameter larger than 50um was counted from three different wells.

Immunoblotting analysis

Immunoblotting was done as described previously(23). Antibodies used in immunoblotting were Gal-1 (Abcam), AR (Abcam), E-cadherin, phospho AKT, AKT, beta-actin (Cell Signaling) and Ras (chemicon). Immunoblotting bands were quantified by Image J software.

Pull-down and immunoprecipitation assay

Pull-down assay was done as described previously(23). For the immunoprecipitation, 10 µL of anti-Gal-1(Abcam) was incubated with 100 µL of slurry of Protein A/G Sepharose (Abcam) for 4 h at 4°C by gently mixing. 1 x 10^6 prostate cancer cells were seeded on the 6 well plates and treated with DMSO or LLS30 10 µM overnight. 22RV1 cells were lysed in a non-denaturing lysis buffer (20 mM Tris-HCl pH 8.0, 137 mM NaCl, 2mM EDTA, 2 mg/mL aprotinin and 2 mg/mL leupeptin) and incubated on ice for 20 min. After centrifugation at 12,000 X g for 20 min at 4℃, total cell lysates were collected. 30 µg of lysate was added in protein/antibody/sepharose mixture at 4°C under rotary agitation overnight. Cell lysates extracted from LLS30-treated and DMSO-treated 22Rv1 were added to the antibody conjugate mixture for 4 h at 4°C.Sepharose were washed with PBS and then elute the beads with 150 mM glycine pH 2.5 for 10 minutes. The eluent was then neutralized by adding 10 mL neutralization buffer (Tris, pH 8.0) and subject to immunoblotting to check the precipitation of proteins.

Immunocytochemistry (ICC)

Cells were fixed in 4% para-formaldehyde. Non-specific protein binding was blocked by adding 5% BSA, and 0.5% Triton X-100 for permeabilization. We used rabbit antihuman galectin-1 (Abcam). Cells were incubated with primary antibody (1:200 in PBS) for overnight at 4°C. After washing with PBS, cells were then incubated with the secondary antibody, an FITC-conjugated goat anti-rabbit IgG (Jackson) for 1 hour at room temperature. Finally, the cells nuclear DNA were stained with DAPI (4',6-Diamidino-2-Phenylindole, Dihydrochloride) (Invitrogen). After washing, the cells were mounted and photographed using a confocal microscope (Zeiss).

Immunohistochemistry (IHC)

Tissue microarray (TMA) sections were de-waxed using xylene twice and rehydrated with 100% ethanol for 5 minutes, 95% and 80% ethanol for 5 minute each. Then rinse in PBS. Antigen retrival was

performed in 10 mM, pH 6.0 sodium citrate buffer at 95-100°C for 20 mins. After cooling down to room temperature, tissue sections were rinsed with PBS once followed by blocking endogenous peroxidase with 1% H_2O_2 and blocking non-specific binding site with Power Block (BioGenex) for 5 min at room temperature each. The tissue sections were then incubated with the specific antibody against Gal-1 (Abcam) or AR-V7 (GeneTex) or E-Cad (Cell signaling) or ki-67 (Cell signaling) overnight, followed by rinsing with PBS and incubation by an biotin-conjugated goat anti-rabbit IgG (BioGenex), as the second antibody. TMA sections were then incubated with strepavidin conjugated-HRP (BioGenex) for 20 mins at room temperature. HRP activity was detected using diaminobenzidine tetrahydrochloride (DAB) as substrate (BioGenex). Nuclei were counterstained with hematoxylin (Cell signaling). The ki-67 positive cells were counted in 3 random chosen areas.

Migration and invasion assays.

In vitro cell migration assays were performed using Trans-well chambers (8 μM pore size)(Costar). were allowed to grow to 80% confluency and were serum-starved for 24 h. 1×10^4 CRPC cells carrying control or Gal-1 siRNA were added to the upper chamber and treated with DMSO or 5 μM LLLS30 in 250μl serum-free medium. Complete medium was added to the bottom wells of the chambers. After 72 h, the cells that had not migrated were removed from the upper face of the filters using cotton swabs, and the lower surfaces of the filters were fixed with 5% glutaraldehyde solution and stained with 0.5% Crystal Violet Staining Solution. The migratory cells were counted in 3 random chosen areas from each membrane in the X10 fields. The cell number was shown by the average of triplicate assays for each experimental condition. Similar inserts coated with Matrigel were used to determine invasiveness of PC3 cells in the invasion assay.

In vivo xenograft tumor and metastasis assays

LLS30 stock solutions (6X) were prepared in 50% absolute alcohol and 50% Tween-80 to make 6 mg/ml and 18 mg/ml for PC3 and 22RV1 xenografts, respectively. Male congenital athymic BALB/c nude (nu/nu) mice were purchased from the Jackson laboratory. Mouse xenograft experimental protocols were approved by the Institutional Animal Care and Use Committee (IACUC) at University of California, Davis. 2×10^6 22RV1 or PC3 cells were subcutaneously injected to the right side of the mouse dorsal flank. The tumors were allowed to grow to about 100 mm^3. In 22RV1 xenograft mouse experiments, mice were randomly divided into control and treatment groups with 6 mice per group.

Mice bearing 22Rv1 xenografts were given a daily I.V. administration for 2 weeks with vehicle control 8.7% alcohol and 8.7% Tween-80 in PBS or 30 mg/kg LLS30 daily. In PC3 xenograft mouse experiments, mice were randomly divided into control and treatment groups with 4 mice per group. PC3 bearing mice were treated with control 8.7% alcohol and 8.7% Tween-80 in PBS or 10 mg/kg LLS30 daily for 5 successive days or 10 mg/kg docetaxel every 3 days for 4 shots or combination of LLS30 and docetaxel via I.V. Tumor size and body weight were measured twice a week and tumor volumes were calculated using (length x width^2)/2. Luciferase-labeled PC3 cells were used for *in vivo* metastasis assays. 2 x 10^6 firefly luciferase-labeled PC3 cells were I.V. injected to male congenital athymic BALB/c nude (nu/nu) mice. Mice received 4.35% alcohol/4.35% Tween-80 vehicle or LLS30 5mg/kg, daily I.V. administration for 5 successive days. Bioluminescence IVIS Imaging System (Caliper LifeSciences) was used to monitor luciferase-expressing cells in mice, 5 min after intraperitoneal injection of 100 mg/kg D-luciferin.

Statistical analysis

Expression level of Gal-1 was scored as follows: 0, negative; 1, low intensity; 2, moderate intensity; 3, high intensity; and 4, very high intensity. Two pathologists have visually scored IHC data. *P* value < 0.05 is considered statistically significant difference. All *in vitro* studies were performed in triplicate in two different experiments.

Results

1. Gal-1 is a powerful target in PCa

The expression level of Gal-1 was examined using immunohistochemistry in 38 BHP and 111 human prostate cancer specimens, including Gleason score≤6 (low-grade or well differentiated), =7 (intermediate-grade or moderately differentiated), and ≥8 (high-grade or poorly differentiated) (22). In support of previous reports (24), the immunostaining results showed that Gal-1 expression level was very low in all non-tumor samples, and highly expressed in prostate cancer tissues (Fig. 1A). Our study showed Gal-1 was progressively upregulated from low-, intermediate- (low vs. intermediate-grade PCa, $p = 0.002$) to high-grade PCa (intermediate- vs. high-grade PCa, $p < 0.001$) (Fig. 1B). This clinical observation indicates the important role of Gal-1 in regulating tumor progression and metastasis.

The CRPC cell lines PC-3, DU-145, 22Rv1 and CWR-R1 expressed very high levels of Gal-1 compared to the androgen dependent LNCaP cells (Fig. 1C). To examine whether Gal-1 regulates PCa cell proliferation and metastasis, Gal-1 knockdown was conducted in Gal-1 expressing CRPC cell lines including PC3 (AR negative), DU145 (AR negative), 22RV1 (AR positive) and CWR-R1 (AR positive) (Fig. 1D). Reduced cell viability was observed in siRNA treated cells that experienced Gal-1 knockdown (Fig. 1E). In addition, several characteristics of the metastatic phenotype including migration, invasion and survival in the anchorage independent state were inhibited upon treatment with siRNA against Gal-1 (Fig. 1F, 1G). Knockdown of Gal-1 by siRNAs significantly inhibited the growth of both AR positive and AR negative cancer cells, suggesting that Gal-1 mediated cell growth through both AR-dependent and AR-independent molecular mechanisms. Taken together these results indicate a very important role for Gal-1 in PCa development and progression.

2. Development of Gal-1 inhibitor LLS30

Through development and implementation of a cell-based ultra high-throughput one-bead two-compound (OB2C) combinatorial screening platform, we have recently identified a small molecule LLS2 as a pro-apoptotic agent and a potent Gal-1 inhibitor (25). Potency of LLS2 is modest, with an IC_{50} of 15-35 μM in most cells tested. We therefore conducted structure-activity relationship (SAR) studies of LLS2; we designed, synthesized and evaluated 30 analogs of LLS2, with modifications on R_1, R_2 and R_3 groups (Supplementary Fig. 1). Among them, LLS30 (structure is shown in Fig. 2A) was identified as the most potent compound. Molecular docking studies suggested the sugar-binding groove

is the predominant binding site for LLS30 (Fig. 2B). The target protein galectin-1 of LLS30 was confirmed by pull down assay (Fig. 2C). Surface plasmon resonance (SPR) binding analysis was further performed to assess the interaction of LLS30 as a solution phase analyte to the immobilized human Gal-1 on a CM5 chip. We observed dose-dependent binding of LLS30 to Gal-1, which was not saturated at the highest tested concentration of 250 μM (Fig. 2D). LLS30 was found to be active against both AR negative cells PC3, DU145, and AR positive cells, 22RV1 and CWR-R1 cells, with an IC_{50} value of 10.4 μM, 5.3 μM, 3.3 μM and 5.9 μM, respectively (Fig. 2E). Gal-1 was not expressed in the androgen sensitive LNCaP cells (Fig. 1C), which is consistent with our observation that LNCaP cells, compared to 22RV1 Gal-1 positive cells, were less sensitive to LLS30 (Fig. 2F), suggesting that LLS30 kills cell via Gal-1 target.

3. LLS30 affects Gal-1 binding affinity to its binding partners through allosteric inhibition of Gal-1

LLS30/Gal-1 interaction was further characterized by circular dichroism (CD) spectroscopy. We observed that the CD spectrum for the LLS30/Gal-1 complex has a substantially different line shape including the shape of the curve (e.g. ratio of the 225/210 nm peaks) and the peak positions, suggesting that the Gal-1 undergoes a significant conformational change upon LLS30 binding (Fig. 3A). Such a change may affect Gal-1 binding affinity to its binding partners. To test this hypothesis, we performed co-immunoprecipitation experiments by detecting RAS, one well-known binding partner of Gal-1. The results showed decreased amount of RAS binding to Gal-1 in LLS30-treated 22Rv1 cells compared to untreated cells (Fig. 3B). As shown in Fig 3C, Gal-1 was localized not only in the cytoplasm and nucleus but also on the cell surface of PC3 cells. Gal-1 has been shown to bind to collagen type I, laminin, and fibronectin (26), we further examined whether LLS30 exhibited any effect on the adhesion of PC3 cells to these proteins. Pretreatment of PC3 cells with LLS30 decreased the number of adherent cells on collagen, fibronectin, laminin coated dishes compared to DMSO treated cells (Fig. 3D). As shown in 3D, LLS30 inhibited the adhesion of PC3 cells to collagen ($76\pm5\%$, $p<0.05$), laminin ($69\pm4\%$, $p<0.05$) and fibronectin ($62\pm12\%$, $p<0.05$). Taken together, these studies indicate that LLS30 binds Gal-1 as an allosteric inhibitor, resulting in a decrease in binding affinity of Gal-1 to its binding partners.

4. Effects of LLS30 on tumor growth is associated with its effect on Gal-1

The RAS and AKT pathways are frequently activated in human advance PCa and have been proposed to promote prostate cancer progression (27-29). Given that Gal-1 is essential to stabilize membrane Ras and thereby induce the activation of Ras (30), we further evaluated whether LLS30 could have an effect on the phosphorylation of Akt. Western blotting of cell lysates collected from CRPC PC3 (AR negative) and 22RV1 (AR positive) cells treated by LLS30 or DMSO showed that LLS30 treatment induced expression of p21, a cyclin-dependent kinase (CDK) inhibitor that interacts with Akt and also regulates survival (Fig. 4A). Phosphorylated AKT was partially suppressed in PC3 and 22RV1 cells after 24 hr treatment with 10 μM LLS30 (Fig. 4A). Correspondingly, decreased expression of phospho-AKT and induced expression of p21 were observed in both PC3 and 22RV1 cells following knockdown of Gal-1 with siRNA (Fig. 4A). Interestingly, treatment with LLS30 as well as siRNA knockdown of Gal-1, also decreased expression of AR and AR-Variants (AR-Vs) in 22RV1 cells (Fig. 4A). These results indicated that LLS30 inhibited CRPC cell growth through the suppression of Akt and AR pathway, and induction of p21. Moreover, these effects are most likely mediated through the inhibition of Gal-1 function. *In vivo* efficacy study showed that LLS30 at 30mg/kg dose significantly reduced the 22RV1 AR positive tumor growth (Fig. 4B, 4C). No adverse effect such as weight loss was observed in mice treated with LLS30. Ki-67 positive cells were down-regulated by 38.8% in LLS30-treated tumor compared with vehicle control (Fig. 4D). Together these results indicate significant efficacy of LLS30 against PCa tumors that is likely caused by Gal-1 inhibition.

5. LLS30 has synergistic anti-tumor activity with docetaxel in CRPC cells

Docetaxel, a chemotherapeutic agent for CRPC patients, binds to microtubules and inhibits the disassembly of microtubules, causing cell cycle arrest at the G_2/M phase. In this study, flow cytometry showed that CRPC PC3 cells accumulated in the G_1/S phase of the cell cycle following 10 μM LLS30 for 24 hr (Fig. 5A). Fig 4A showed that LLS30 treatment induced expression of p21, a CDK inhibitor supporting G_1/S arrest. In addition to cell cycle arrest, LLS30 triggered apoptosis in PC3 cells treated with LLS30 10 μM for 72 hours (Fig. 5B). It has been known that the combination drug regimens that drugs used in combination work at different stage of cell cycle are most effective(31, 32). LLS30 may exert the maximum cytotoxic effect when it combines with docetaxel causing G2/M arrest. Thus, the combinatorial effects of LLS30 and docetaxel on CRPC PC3 and 22RV1 cells were assessed. Combination studies showed that LLS30 can potentiate the antitumor effects of docetaxel in PC3 and 22RV1 cells (Fig. 5C). Furthermore, decreased phospho-AKT expression was observed after combined

LLS30/docetaxel treatment (Fig. 5D), and it was further confirmed by immunoblot analysis (Fig. 5E). *In vivo* study showed that LLS30 at 10mg/kg dose significantly suppressed the growth of PC3 tumor, and combination of LLS30 with docetaxel caused complete tumor regression that did not recover in 24 days (Fig. 5F, 5G). Moreover, ki-67 positive cells were down-regulated in LLS30-treated and further down-regulated in combination LLS30/docetaxel treated tumor (Fig. 5H). Systemic toxicity of the compound – alone or in combination with docetaxel was evaluated in mice by measuring liver and kidney function tests, which were found to be within acceptable range (Supplementary Table 1). Furthermore, no weight loss was observed in all treated mice, indicating low toxicity for this compound.

6. LLS30 inhibited PCa metastasis and reverse EMT *in vivo*

Noticeably, histological analysis of the resected tumor revealed that many round cells were present (Fig. 5G), suggesting that LLS30 plays an inhibitory role in prostate cancer invasion. Thus, we investigated the metastasis inhibitory function of LLS30 in metastatic PC3 cells. We performed genome-wide gene expression analysis by comparing PC3 cells treated with 10 μM LLS30 as early as 30 minutes and up to 24 hours (Supplementary Table 2). Functional pathway analysis performed in the genes downregulated (<1.5-fold and $p<0.05$) by LLS30 revealed the most prominently altered pathways were the migration and invasion related signaling pathway, which includes PI3K-AKT, focal adhesion, extracellular matrix (ECM)-receptor as well as α6β1 and α6β4 integrin signaling pathway (Fig. 6A, 6B, Supplementary Table 3). Immunoblotting assays confirmed the suppression of the expression of integrin α6, β4, and β1 (Fig. 6C). The phosphorylation of FAK, a downstream kinase of integrin, was reported to control aggressive phenotype of androgen-independent PCa cells (33). Expression of phospho-FAK was also suppressed by LLS30 (Fig. 6C). In addition, treatment with LLS30 in PC3 cells made cells morphologically express more epithelial features including increased cell-cell contact and fewer lamellipodial protrusion, and it also remarkably increased expression of E-cadherin, a molecular mark for epithelial characteristics (Fig. 6D). Trans-well migration assay showed that LLS30 inhibited PC3 cells migration and invasion *in vitro* (Fig. 6E). Next, the invasion-inhibitory activity of LLS30 was measured *in vivo*. We transplanted luciferase-tagged PC3 cells into nude mice via tail-vein injection, followed by LLS30 treatment (5mg/kg q.d.X5) two weeks later (Fig. 6F). In control groups, metastatic colonization was observed in all 6 mice in a period of six weeks after injection (Fig. 6G). The metastatic patterns are consistent with the previous studies(34, 35), PC3 cells are spread to major visceral organs, such as kidneys, lungs, livers, and spleens. In LLS30 treated group, only 1 mouse developed metastases

(Fig. 6G). These results indicated that LLS30 is capable of inhibiting tumor invasion and metastasis *in vivo*.

Discussion

The majority of PCa patients who are treated with ADT will eventually develop CRPC, typically either docetaxel, CYP17A1 inhibitor abiraterone, or AR inhibitor enzalutamide is used to treat CRPC after ADT has failed (36-39). However, rapid resistance to these treatments is commonly developed following prolonged use in CRPC patients (40, 41). Thus, there are no effective durable therapies for patients with CRPC. AR is the most important driver of CRPC development and of acquired resistance to drugs, while AR-independent signal pathway can also contribute to CRPC and drug resistance (42). In this study, we have reported that Gal-1 protein was expressed only in CRPC cells but not in androgen-sensitive LNCaP cells (Fig. 1C). Importantly, knockdown of Gal-1 by siRNAs significantly reduced cell viability of both AR positive and AR negative cancer cells (Fig. 1E), providing evidence that Gal-1 controls PCa growth through both AR-dependent and AR-independent pathways. Therefore, the application of Gal-1-targeting therapy deserves attention. This study provides the molecular rationale for the use of Gal-1 inhibitors, such as LLS30, in the treatment of AR-driven, as well as non-AR-driven, CRPC.

It has been reported that expression of AR-Vs is associated with resistance to enzalutamide and abiraterone (43, 44). Our results revealed that Gal-1 knockdown suppressed both AR and AR-Vs expression in 22RV1 cells which is AR-Vs expressing cells (Fig. 4A). Treatment with LLS30 recapitulated siGal-1–mediated reduction of AR and AR-Vs (Fig. 4A). It implied that Gal-1 plays a role in regulating AR and AR-Vs expression. Suppression of AR-Vs by Gal-1 knockdown or LLS30 may re-sensitizes resistant cells to abiraterone or enzalutamide treatment.

Elevated Gal-1 has previously been found to be associated with progression to the metastatic state in various cancers. In epithelial ovarian cancer tissues, Gal-1 upregulated c-Jun, matrix metalloproteinase-9 (MMP-9), Bcl-2, and p21 expression through activation of the H-Ras/Raf/extracellular signal-regulated kinase (ERK) pathway (45). Gal-1 mediates lung cancer metastasis by potentiating integrin α6β4 and the Notch1/Jagged2 signaling pathway (15). Gal-1 increased the secretion of stromal cell-derived factor-1 (SDF-1) through activation of NF-κB, and promoted pancreatic cancer metastasis (16). Gal-1 is also involved in tumor invasion by increasing MMP expression and reorganizing cytoskeletons in oral cancers and lung adenocarcinoma (17). Thus, it is logical that inhibition of Gal-1 expression or function may reduce the metastatic character of certain cancer cells. Indeed, the results in this study showed that

suppression of Gal-1 in PC3 and 22RV1 CRPC cells resulted in reduction of the cell migration and invasion associated with metastasis (Fig. 1F).

No Gal-1 inhibitors have been approved to date for clinic use in patients due to lack of potent, specific and *in vivo* effective molecules (21). LLS30 is a benzimidazole-based small molecule with distinct structural differences from the established Gal-1 inhibitor OTX008 (46, 47). Moreover, LLS30 is more potent than OTX008 on CRPC cells (Supplementary Fig. 2). Akt and AR pathway are important oncogenic signaling pathways in human PCa(29, 48). This study showed that LLS30 is able to suppress the Akt and AR pathways resulting in the growth inhibition of CRPC cells.

ADT causes cell cycle arrest in G_0/early G_1-phase (49, 50) and docetaxel causes a G_2/M arrest. However, cancer cells can develop resistance to these treatments. Combination with another cell cycle based agent could overcome the associated resistance and thus increase the potency of treatment (31, 32). Indeed, in this study we have shown that LLS30 induced G_1/S arrest and apoptosis (Fig. 5A, 5B), contributing to the whole combination effect with docetaxel (Fig. 5C, 5F, 5G). In addition to drug synergy with docetaxel, combination of LLS30 to ADT for PCa patients may prevent CRPC development and have a significant impact on overall survival. Further studies to investigate the combination effects of LLS30 and ADT are currently ongoing.

Integrins are large complex transmembrane glycoproteins that provide anchorage for cell motility and invasion (51, 52). It has been reported that ligation of integrins with extracellular matrix components activates FAK or c-Src kinases, resulting in promotion of cell motility, cell cycle progression and cell survival (53). Tumor cell expression of the integrins α5β1, α9β1, αvβ3, α6β4, and αvβ5 has been correlated with metastatic features in melanoma, breast carcinoma and lung cancers (9,10). The role of Gal-1 in regulating integrin α6β4 and FAK in lung cancer cells has been confirmed by Hsu *et al* (15). In prostate cancer, Cress et al. reported that the upregulation of α6β1 and laminin contributes to the invasive phenotype (54). Yoshioka *et al*. also observed overexpression of integrin β4 protein in 35% of invasive PCa (55). LLS30 is a Gal-1 selectively allosteric inhibitor (Fig. 3) and our cDNA microarray data showed LLS30 treatment downregulated the number of genes that are associated with focal adhesion-, integrin α6β1, and α6β4 pathways (Fig. 6A, 6B). The altered expressions of phosphor-FAK, integrin α6, β1 and β4 by LLS30 have been confirmed (Fig. 6C). As shown in Fig. 6H, LLS30 is capable of inhibiting tumor invasion and metastasis *in vitro* and *in vivo* (Fig. 6E, 6F, 6H), which might be ascribed to inhibition of Gal-1 function and its downstream intergrin/FAK pathway.

Gal-1 has previously been reported to induce tumor angiogenesis (56) and T cell apoptosis (57). Gal-1 accumulates in the cancer-associated stroma and may act as an immunological shield by inducing activated T-cell apoptosis to help tumors escape from immune attack (18). A recent study reports that the immune checkpoint regulator PD-L1 is highly expressed in aggressive PCa (58). We therefore hypothesize that LLS30 can augment the therapeutic efficacy of immune checkpoint inhibitors, such as nivolumab, pembrolizumab and avelumab, in mCRPC patients. Work is currently underway in our laboratory to explore this hypothesis. In addition, Gal-1 is a potential therapeutic target for HIV (59, 60), autoimmune disorders (61), and obesity (62). Developed in this study LLS30 exhibits favorable pharmacokinetic parameters (Supplementary Fig. 3), is not toxic, and may also be applicable to diseases with Gal-1 overexpression.

In conclusion, highly expression of Gal-1 in PCa functionally promotes tumor progression and metastasis, and is an important target for mCRPC therapy. Importantly, we have developed a novel Gal-1 selective allosteric small molecule inhibitor, LLS30; it is a promising compound that can potentiate the anti-tumor effect of docetaxel and inhibit metastasis *in vivo*. LLS30/docetaxel combination treatment may serve as potential novel therapeutic approach to treat CRPC patients.

Acknowledgments:

This work was supported by grants of the NIH (2R33 CA160132, to Dr. K. S. Lam). Thanks lab support from Dr. P. M. Ghosh lab (I01BX000400 from the Department of Veterans Affairs and R01CA185509 from the NIH), and from Dr. Y. Duan lab (R01GM079383 from the NIH). The Combinatorial Chemistry Shared Resource at University of California Davis assists the synthesis of LLS30, utilization of this Shared Resource was supported by the UC Davis Comprehensive Cancer Center Support Grant NCI P30CA093373, and the Gene Expression BeadChip analysis was carried out at the DNA Technologies and Expression Analysis Cores at the UC Davis Genome Center, and the authors also acknowledge the Campus Mass Spectrometry facility, the NMR facility, and the PK/PD Bio-analytical Core Facility at UC Davis. The authors also thank Dr. Allen C. Gao, Dr. Christopher P. Evans and Dr. Joy C Yang, for valuable input on an earlier version of the manuscript, and thank Tissue Bank at Chang Gung Memorial Hospital, Keelung for staining technical support.

References

1. Siegel RL, Miller KD, Jemal A. Cancer statistics, 2017. CA Cancer J Clin. 2017;67:7-30.
2. Huggins C HC. The effect of castration, of estrogen and of androgen injection on serum phosphatases in metastatic carcinoma of the prostate. Cancer Res. 1941;1:293-7.
3. Cookson MS, Roth BJ, Dahm P, Engstrom C, Freedland SJ, Hussain M, et al. Castration-Resistant Prostate Cancer: AUA Guideline. The Journal of urology. 2013;190:429-38.
4. Zhang P, Zhang P, Shi B, Zhou M, Jiang H, Zhang H, et al. Galectin-1 overexpression promotes progression and chemoresistance to cisplatin in epithelial ovarian cancer. Cell death & disease. 2014;5:e991.
5. Carlini MJ, Roitman P, Nunez M, Pallotta MG, Boggio G, Smith D, et al. Clinical relevance of galectin-1 expression in non-small cell lung cancer patients. Lung Cancer. 2014;84:73-8.
6. Jung EJ, Moon HG, Cho BI, Jeong CY, Joo YT, Lee YJ, et al. Galectin-1 expression in cancer-associated stromal cells correlates tumor invasiveness and tumor progression in breast cancer. International journal of cancer Journal international du cancer. 2007;120:2331-8.
7. White NM, Masui O, Newsted D, Scorilas A, Romaschin AD, Bjarnason GA, et al. Galectin-1 has potential prognostic significance and is implicated in clear cell renal cell carcinoma progression through the HIF/mTOR signaling axis. Br J Cancer. 2014;110:1250-9.
8. Martinez-Bosch N, Fernandez-Barrena MG, Moreno M, Ortiz-Zapater E, Munne-Collado J, Iglesias M, et al. Galectin-1 Drives Pancreatic Carcinogenesis through Stroma Remodeling and Hedgehog Signaling Activation. Cancer Res. 2014.
9. Liu FT, Rabinovich GA. Galectins as modulators of tumour progression. Nat Rev Cancer. 2005;5:29-41.
10. Perillo NL, Pace KE, Seilhamer JJ, Baum LG. Apoptosis of T cells mediated by galectin-1. Nature. 1995;378:736-9.
11. Rubinstein N, Alvarez M, Zwirner NW, Toscano MA, Ilarregui JM, Bravo A, et al. Targeted inhibition of galectin-1 gene expression in tumor cells results in heightened T cell-mediated rejection. Cancer Cell. 2004;5:241-51.
12. Fischer C, Sanchez-Ruderisch H, Welzel M, Wiedenmann B, Sakai T, André S, et al. Galectin-1 Interacts with the α5β1 Fibronectin Receptor to Restrict Carcinoma Cell Growth via Induction of p21 and p27. J Biol Chem. 2005;280:37266-77.
13. Wells V, Davies D, Mallucci L. Cell cycle arrest and induction of apoptosis by beta galactoside binding protein (beta GBP) in human mammary cancer cells. A potential new approach to cancer control. Eur J Cancer. 1999;35:978-83.
14. Stanley P. Galectin-1 Pulls the Strings on VEGFR2. Cell. 2014;156:625-6.

15. Hsu YL, Wu CY, Hung JY, Lin YS, Huang MS, Kuo PL. Galectin-1 promotes lung cancer tumor metastasis by potentiating integrin alpha6beta4 and Notch1/Jagged2 signaling pathway. Carcinogenesis. 2013;34:1370-81.
16. Qian D, Lu Z, Xu Q, Wu P, Tian L, Zhao L, et al. Galectin-1-driven upregulation of SDF-1 in pancreatic stellate cells promotes pancreatic cancer metastasis. Cancer Lett. 2017;397:43-51.
17. Wu M-H, Hong T-M, Cheng H-W, Pan S-H, Liang Y-R, Hong H-C, et al. Galectin-1-Mediated Tumor Invasion and Metastasis, Up-Regulated Matrix Metalloproteinase Expression, and Reorganized Actin Cytoskeletons. Mol Cancer Res. 2009;7:311-8.
18. A F, BruÃle vd, Castronovo DWaV. Increased expression of galectin-1 in carcinoma-associated stroma predicts poor outcome in prostate carcinoma patients. J Pathol. 2001;193:80-7.
19. Laderach DJ, Gentilini LD, Giribaldi L, Delgado VC, Nugnes L, Croci DO, et al. A Unique Galectin Signature in Human Prostate Cancer Progression Suggests Galectin-1 as a Key Target for Treatment of Advanced Disease. Cancer Res. 2013;73:86-96.
20. Shih T-C, Liu R, Fung G, Bhardwaj G, Ghosh PM, Lam KS. A Novel Galectin-1 Inhibitor Discovered through One-Bead-Two-Compounds Library Potentiates the Anti-tumor Effects of Paclitaxel in vivo. Mol Cancer Ther. 2017.
21. Blanchard H, Bum-Erdene K, Bohari MH, Yu X. Galectin-1 inhibitors and their potential therapeutic applications: a patent review. Expert Opin Ther Pat. 2016;26:537-54.
22. Epstein JI, Allsbrook WCJ, Amin MB, Egevad LL, Committee atIG. The 2005 International Society of Urological Pathology (ISUP) Consensus Conference on Gleason Grading of Prostatic Carcinoma. The American Journal of Surgical Pathology. 2005;29:1228-42.
23. Hsieh SY, Shih TC, Yeh CY, Lin CJ, Chou YY, Lee YS. Comparative proteomic studies on the pathogenesis of human ulcerative colitis. Proteomics. 2006;6:5322-31.
24. Laderach DJ, Gentilini LD, Giribaldi L, Delgado VC, Nugnes L, Croci DO, et al. A unique galectin signature in human prostate cancer progression suggests galectin-1 as a key target for treatment of advanced disease. Cancer Res. 2013;73:86-96.
25. Shih T-C, Liu R, Fung G, Bhardwaj G, Ghosh PM, Lam KS. A Novel Galectin-1 Inhibitor Discovered through One-Bead Two-Compound Library Potentiates the Antitumor Effects of Paclitaxel *in vivo*. Mol Cancer Ther. 2017;16:1212-23.
26. Moiseeva EP, Williams B, Samani NJ. Galectin 1 inhibits incorporation of vitronectin and chondroitin sulfate B into the extracellular matrix of human vascular smooth muscle cells. Biochimica et Biophysica Acta (BBA) - General Subjects. 2003;1619:125-32.
27. Kinkade CW, Castillo-Martin M, Puzio-Kuter A, Yan J, Foster TH, Gao H, et al. Targeting AKT/mTOR and ERK MAPK signaling inhibits hormone-refractory prostate cancer in a preclinical mouse model. The Journal of clinical investigation. 2008;118:3051-64.

28. Sarker D, Reid AHM, Yap TA, de Bono JS. Targeting the PI3K/AKT Pathway for the Treatment of Prostate Cancer. Clin Cancer Res. 2009;15:4799-805.
29. Malik SN, Brattain M, Ghosh PM, Troyer DA, Prihoda T, Bedolla R, et al. Immunohistochemical Demonstration of Phospho-Akt in High Gleason Grade Prostate Cancer. Clin Cancer Res. 2002;8:1168-71.
30. Paz A, Haklai R, Elad-Sfadia G, Ballan E, Kloog Y. Galectin-1 binds oncogenic H-Ras to mediate Ras membrane anchorage and cell transformation. Oncogene. 2001;20:7486-93.
31. Deep G, Agarwal R. New Combination Therapies with Cell Cycle Agents. Current opinion in investigational drugs (London, England : 2000). 2008;9:591-604.
32. ZALATNAI A. Potential Role of Cell Cycle Synchronizing Agents in Combination Treatment Modalities of Malignant Tumors. In Vivo. 2005;19:85-91.
33. Johnson TR, Khandrika L, Kumar B, Venezia S, Koul S, Chandhoke R, et al. Focal Adhesion Kinase Controls Aggressive Phenotype of Androgen-Independent Prostate Cancer. Mol Cancer Res. 2008;6:1639-48.
34. Das R, Gregory PA, Fernandes RC, Denis I, Wang Q, Townley SL, et al. MicroRNA-194 promotes prostate cancer metastasis by inhibiting SOCS2. Cancer Res. 2016.
35. Stangelberger A, Schally AV, Varga JL, Zarandi M, Szepeshazi K, Armatis P, et al. Inhibitory Effect of Antagonists of Bombesin and Growth Hormone-Releasing Hormone on Orthotopic and Intraosseous Growth and Invasiveness of PC-3 Human Prostate Cancer in Nude Mice. Clin Cancer Res. 2005;11:49-57.
36. Tannock IF, de Wit R, Berry WR, Horti J, Pluzanska A, Chi KN, et al. Docetaxel plus prednisone or mitoxantrone plus prednisone for advanced prostate cancer. N Engl J Med. 2004;351:1502-12.
37. de Bono JS, Oudard S, Ozguroglu M, Hansen S, Machiels JP, Kocak I, et al. Prednisone plus cabazitaxel or mitoxantrone for metastatic castration-resistant prostate cancer progressing after docetaxel treatment: a randomised open-label trial. Lancet. 2010;376:1147-54.
38. de Bono JS, Logothetis CJ, Molina A, Fizazi K, North S, Chu L, et al. Abiraterone and increased survival in metastatic prostate cancer. The New England journal of medicine. 2011;364:1995-2005.
39. Scher HI, Fizazi K, Saad F, Taplin ME, Sternberg CN, Miller K, et al. Increased survival with enzalutamide in prostate cancer after chemotherapy. The New England journal of medicine. 2012;367:1187-97.
40. Claessens F, Helsen C, Prekovic S, Van den Broeck T, Spans L, Van Poppel H, et al. Emerging mechanisms of enzalutamide resistance in prostate cancer. Nature Reviews Urology. 2014;11:712.
41. Attard G, Antonarakis ES. AR aberrations and resistance to abiraterone or enzalutamide. Nature Reviews Urology. 2016;13:697.

42. Karantanos T, Corn PG, Thompson TC. Prostate cancer progression after androgen deprivation therapy: mechanisms of castrate resistance and novel therapeutic approaches. Oncogene. 2013;32:5501.
43. Mostaghel EA, Marck BT, Plymate S, Vessella R, Balk S, Matsumoto AM, et al. Resistance to CYP17A1 inhibition with abiraterone in castration resistant prostate cancer: Induction of steroidogenesis and androgen receptor splice variants. Clinical cancer research : an official journal of the American Association for Cancer Research. 2011;17:5913-25.
44. Li Y, Chan SC, Brand LJ, Hwang TH, Silverstein KAT, Dehm SM. Androgen receptor splice variants mediate enzalutamide resistance in castration-resistant prostate cancer cell lines. Cancer Res. 2013;73:483-9.
45. Zhang P, Zhang P, Shi B, Zhou M, Jiang H, Zhang H, et al. Galectin-1 overexpression promotes progression and chemoresistance to cisplatin in epithelial ovarian cancer. Cell Death Dis. 2014;5:e991.
46. Astorgues-Xerri L, Riveiro ME, Tijeras-Raballand A, Serova M, Rabinovich GA, Bieche I, et al. OTX008, a selective small-molecule inhibitor of galectin-1, downregulates cancer cell proliferation, invasion and tumour angiogenesis. Eur J Cancer. 2014;50:2463-77.
47. Dings RPM, Miller MC, Nesmelova I, Astorgues-Xerri L, Kumar N, Serova M, et al. Antitumor Agent Calixarene 0118 Targets Human Galectin-1 as an Allosteric Inhibitor of Carbohydrate Binding. J Med Chem. 2012;55:5121-9.
48. Chang L, Graham PH, Ni J, Hao J, Bucci J, Cozzi PJ, et al. Targeting PI3K/Akt/mTOR signaling pathway in the treatment of prostate cancer radioresistance. Critical Reviews in Oncology / Hematology. 2015;96:507-17.
49. Knudsen KE, Arden KC, Cavenee WK. Multiple G1 Regulatory Elements Control the Androgen-dependent Proliferation of Prostatic Carcinoma Cells. J Biol Chem. 1998;273:20213-22.
50. Agus DB, Cordon-Cardo C, Fox W, Drobnjak M, Koff A, Golde DW, et al. Prostate Cancer Cell Cycle Regulators: Response to Androgen Withdrawal and Development of Androgen Independence. JNCI: Journal of the National Cancer Institute. 1999;91:1869-76.
51. Ruoslahti E. Integrins. J Clin Invest. 1991;87:1-5.
52. Hynes RO. Integrins: Versatility, modulation, and signaling in cell adhesion. Cell. 1992;69:11-25.
53. Mitra SK, Schlaepfer DD. Integrin-regulated FAK–Src signaling in normal and cancer cells. Curr Opin Cell Biol. 2006;18:516-23.
54. Cress AE, Rabinovitz I, Zhu W, Nagle RB. The α6β1 and α6β4 integrins in human prostate cancer progression. Cancer Metastasis Rev. 1995;14:219-28.
55. Yoshioka T, Otero J, Chen Y, Kim Y-M, Koutcher JA, Satagopan J, et al. β4 Integrin signaling induces expansion of prostate tumor progenitors. The Journal of clinical investigation. 2013;123:682-99.

56. Thijssen VL, Postel R, Brandwijk RJ, Dings RP, Nesmelova I, Satijn S, et al. Galectin-1 is essential in tumor angiogenesis and is a target for antiangiogenesis therapy. Proc Natl Acad Sci U S A. 2006;103:15975-80.

57. Perillo NL, Pace KE, Seilhamer JJ, Baum LG. Apoptosis of T cells mediated by galectin-1. Nature 378,. 1995;378:736 - 9.

58. Gevensleben H, Dietrich D, Golletz C, Steiner S, Jung M, Thiesler T, et al. The Immune Checkpoint Regulator PD-L1 Is Highly Expressed in Aggressive Primary Prostate Cancer. Clin Cancer Res. 2016;22:1969-77.

59. St-Pierre C, Ouellet M, Giguere D, Ohtake R, Roy R, Sato S, et al. Galectin-1-specific inhibitors as a new class of compounds to treat HIV-1 infection. Antimicrobial agents and chemotherapy. 2012;56:154-62.

60. Sato S, Ouellet M, St-Pierre C, Tremblay MJ. Glycans, galectins, and HIV-1 infection. Annals of the New York Academy of Sciences. 2012;1253:133-48.

61. Salatino M, Croci DO, Bianco GA, Ilarregui JM, Toscano MA, Rabinovich GA. Galectin-1 as a potential therapeutic target in autoimmune disorders and cancer. Expert opinion on biological therapy. 2008;8:45-57.

62. Mukherjee R, Kim SW, Park T, Choi MS, Yun JW. Targeted inhibition of galectin 1 by thiodigalactoside dramatically reduces body weight gain in diet-induced obese rats. International journal of obesity. 2015;39:1349-58.

Figure legend

Figure 1. Gal-1 expression in human prostate cancer samples.

(A) The expression levels of Gal-1were detected by IHC (magnification 400 x). (B) Gal-1 expression in 38, 32, 24 and 55 samples of BHP, low-, intermediate- and high-grade PCa tissues, respectively. a: BHP, b: low-, c: intermediate-, d: high-grade. Sampling distribution of Gal-1 expression was displayed by Box-Plot (dash line: mean; lines above and below the dash line, third quartile to the first quartile; lines above and below the box, maximum and minimum). (C) Immunoblots demonstrate the endogenous Gal-1 expression in PCa cells. (D) Suppression of endogenous Gal-1 expression by siRNA by a pool of two different siRNAs in PCa cells. (E) PCa cells transfected with 50 nM scramble control siRNA or siRNA against Gal-1, cell survival was measured at 72 hr post siRNA transfection. (F) Representative image and quantification of Transwell migration and invasion assays. (G) Representative images and quantification of tumor sphere formation of PCa siControl and siGal-1 cells after 10 days post siRNA transfection. *P < 0.05, **P < 0.01, ***P < 0.001; Student's t test, n = 3. Data shown are mean ± s.d.

Figure 2. Novel Gal-1 inhibitor, LLS30.

(A) Chemical structure of LLS30. (B) Computer modeling shows that LLS30 binds the sugar binding groove of the Gal-1 dimer. (C) Pull-down assay to confirm the target protein of LLS30. (D) LLS30/Gal-1 interaction was characterized by SPR. (E) *In vitro* antiproliferative activity of LLS30 in CRPC cells. (F) Proliferation assay of 22Rv1 Gal-1 positive cells and LNCaP Gal-1 negative cells with 6.25 μM LLS30 for 48 hr. Data shown are mean ± s.d.

Figure 3. LLS30 binds to Gal-1 and decreases the binding affinity to its ligand.

(A) CD spectra of Gal-1/LLS30 (18 μM, 50 μM) in 10mM PBS, 5% DMSO, pH = 7.4 buffer. Spectra were an average of 3 spectra, and respective background spectra were subtracted accordingly. (B) Co-immunoprecipitation expertiments showing interaction between Gal-1 and RAS after LLS30 or vehicle treatment. LLS30-treated and DMSO-treated 22Rv1 cells were immunoprecipitated with anti-Gal-1 antibody. Eluted proteins were analyzed by SDS-PAGE and immunoblotted with Gal-1 and RAS antibodies. Input: total protein extracted from LLS30-treated and vehicle-treated 22Rv1 cells were not immunoprecipitated with anti-Gal-1 antibody (C) Immunostaining showed that Gal-1 was localized

in nucleus, cytoplasm and plasma membrane. (D) LLS30 inhibited the adhesion of PC3 cells to collagen, fibronectin and laminin. *P < 0.05, **P < 0.01; Student's t test, n = 3. Data shown are mean ± s.d.

Figure 4. The effects of LLS30 in CRPC cells *in vitro* and *in vivo*.

(A) PC3 and 22RV1 PCa cells treatment with 0.1% DMSO or 10 μM LLS30 or 50nM control siRNA or siRNA against Gal-1, and cell lysates were prepared at 24 hr. (B) Tumor growth curves (n=6). Effect of LLS30 on growth of 22RV1 AR positive tumor xenografts *in vivo*.(C) Tumor weight of the xenografts in inoculated nude mice. (D) H&E, ki-67 stained images (left) and quantification of immunostaining of ki-67 positive cells (right). The cells were counted in 3 random chosen areas. **P < 0.01, ***P< 0.001. Student's t test, n = 3. Data shown are mean ± s.d.

Figure 5. LLS30 can potentiate the anticancer effects of docetaxel *in vitro* and *in vivo*.

(A) Cell cycle analysis for PC-3 cells. Cells were plated and after 24 hours treated with 0.1% DMSO or 10 μM LLS30 after 24 hr, and subjected to cell cycle analysis, and (B) apoptosis was induced after treatment with LLS30 10 μM for 72 hours. (C) LLS30 can potentiate the anticancer effects of docetaxel in CRPC PC3 and 22RV1 cells. (D) Immunofluorescent images and (E) Immunoblots showed the expression of phosphor-AKT was downregulated after combination treatment (LLS30, 10 μM and and docetaxel, 1 nM) in PC3 cells. (F) Pictorial depiction of the effect of the combination LLS30 and docetaxel treatment on the back of a nude mouse at days 0, 12 and 24. (G) Tumor growth curves (n=4). (H) H&E and ki-67 stained images. Data shown are mean ± s.d. ***P< 0.001.

Figure 6. LLS30 inhibited PCa metastasis *in vitro* and *in vivo*.

(A) Heat map of the 20 deregulated genes (<1.5-fold and p < 0.05) in PC3 cells. (B) Functional pathways were analyzed using KEGG & NCI database. (C) Immunoblots showed the expression of phosphor-FAK, integrin alpha6, beta4, and beta1 were downregulated after treatment with LLS30 10 μM for 24 hour in PC3 cells. (D) Morphology of PC-3 and E-cadherin expression after 24 hours treated with DMSO or 5 μM LLS30. (E) Representative image and quantification of of Transwell migration and invasion assays. (F) Time-line of LLS30 therapeutic delivery experiment. (G) IVIS imaging system showing representative nude mice implanted with PC3 cells after treatment with DMSO or LLS30 5mg/kg, daily I.V. administration for 5 successive days. **P < 0.01. Student's t test, n = 3. Data shown are mean ± s.d.

Figure 1

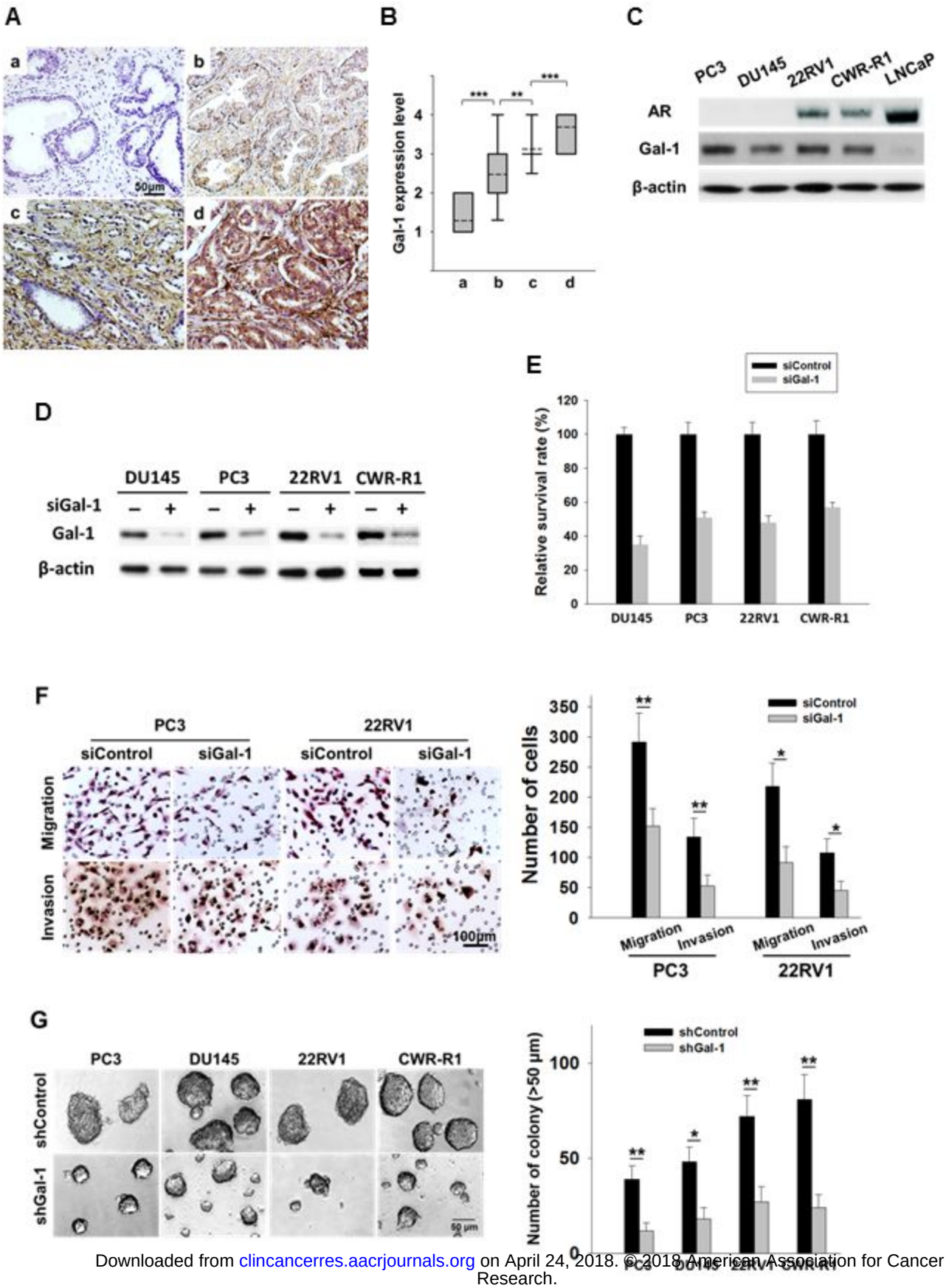

Figure 2

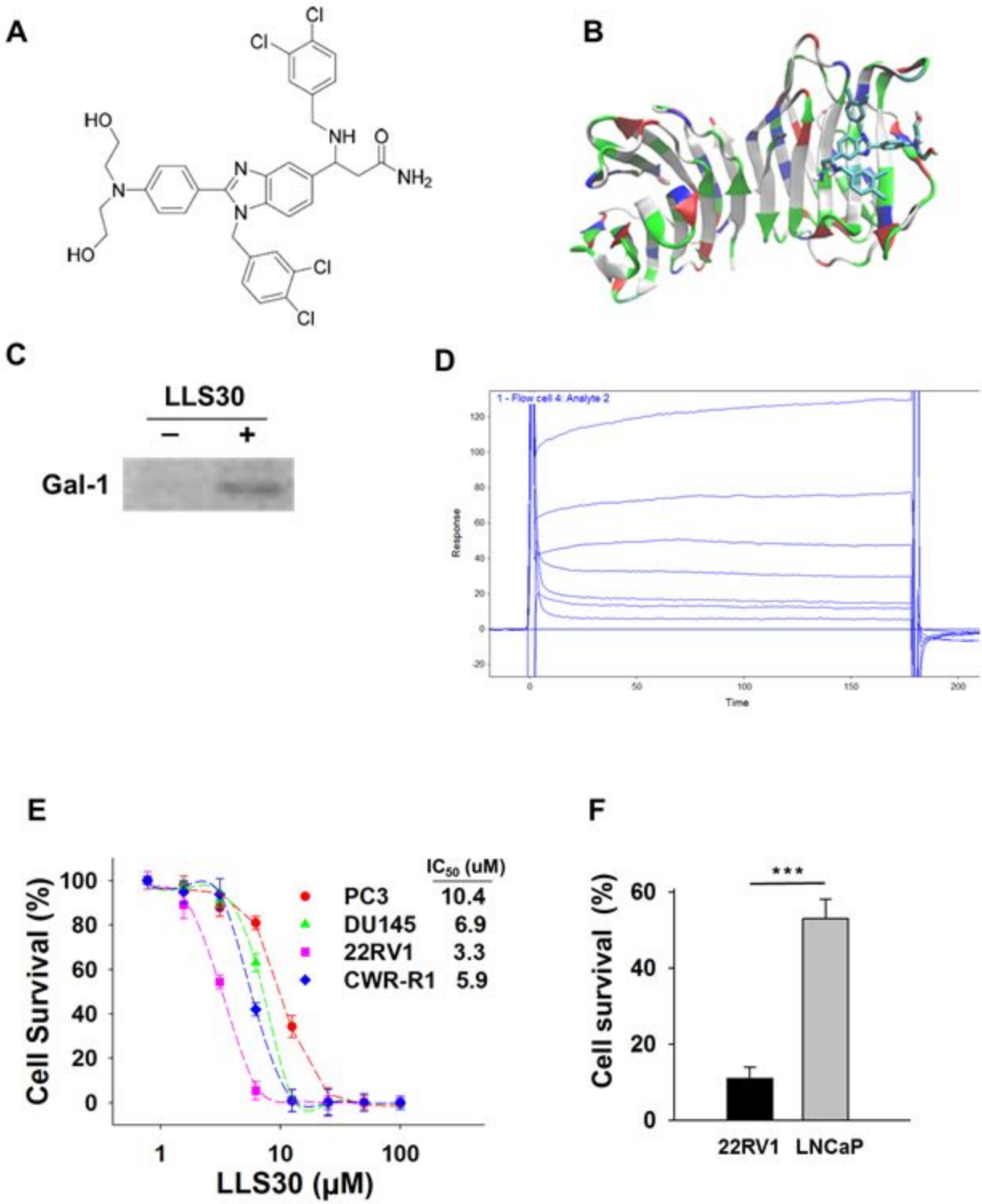

Figure 3

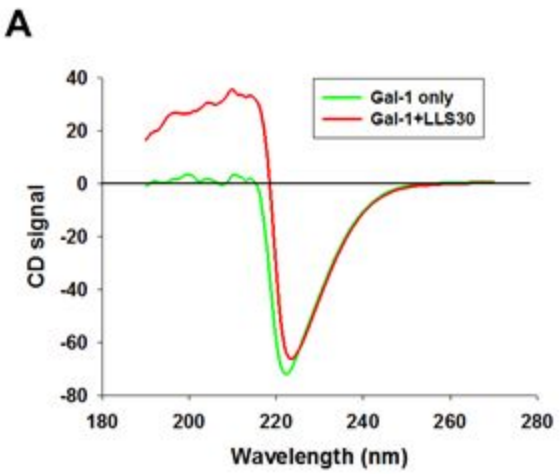

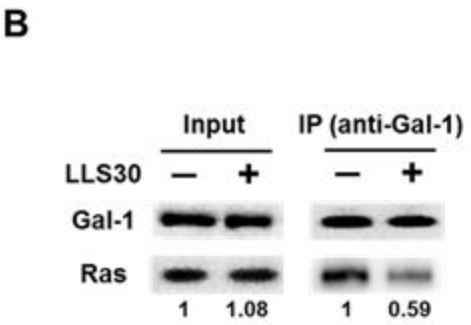

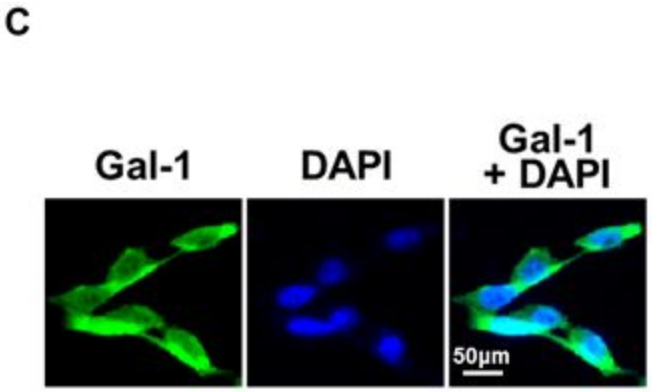

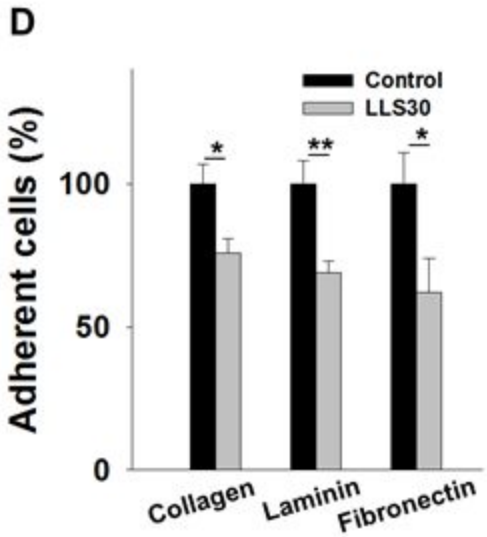

Figure 4

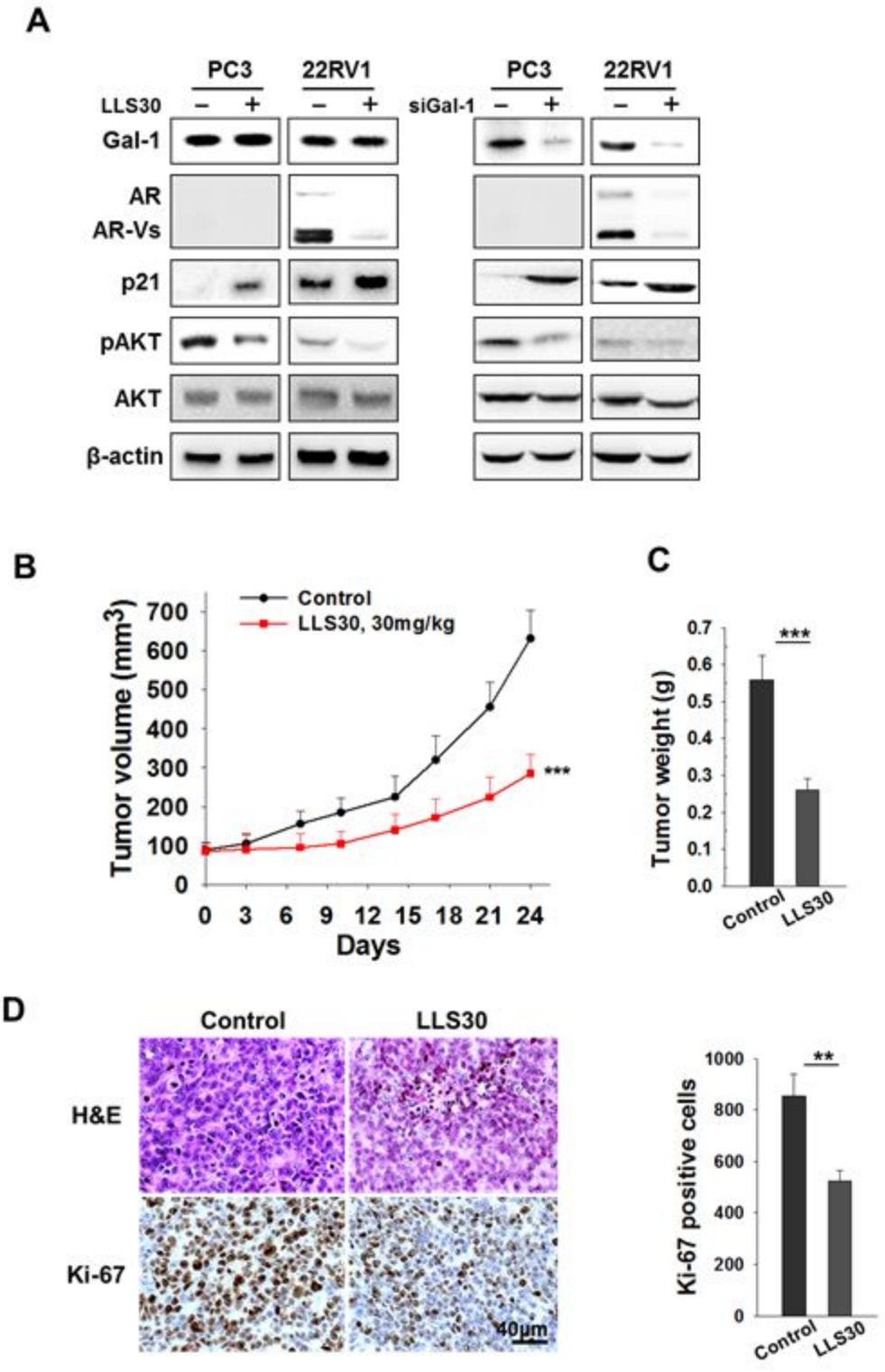

Figure 5

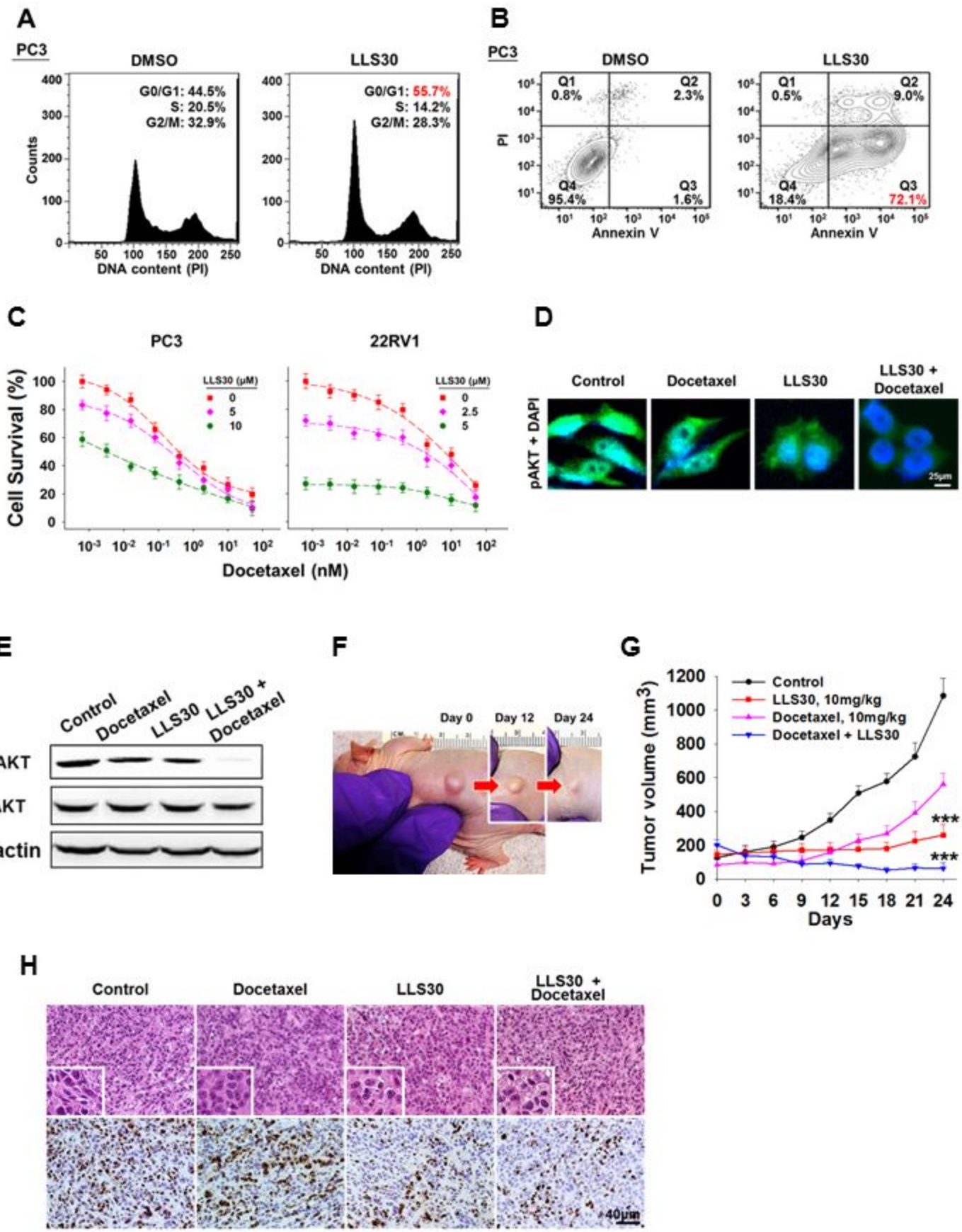

Figure 6

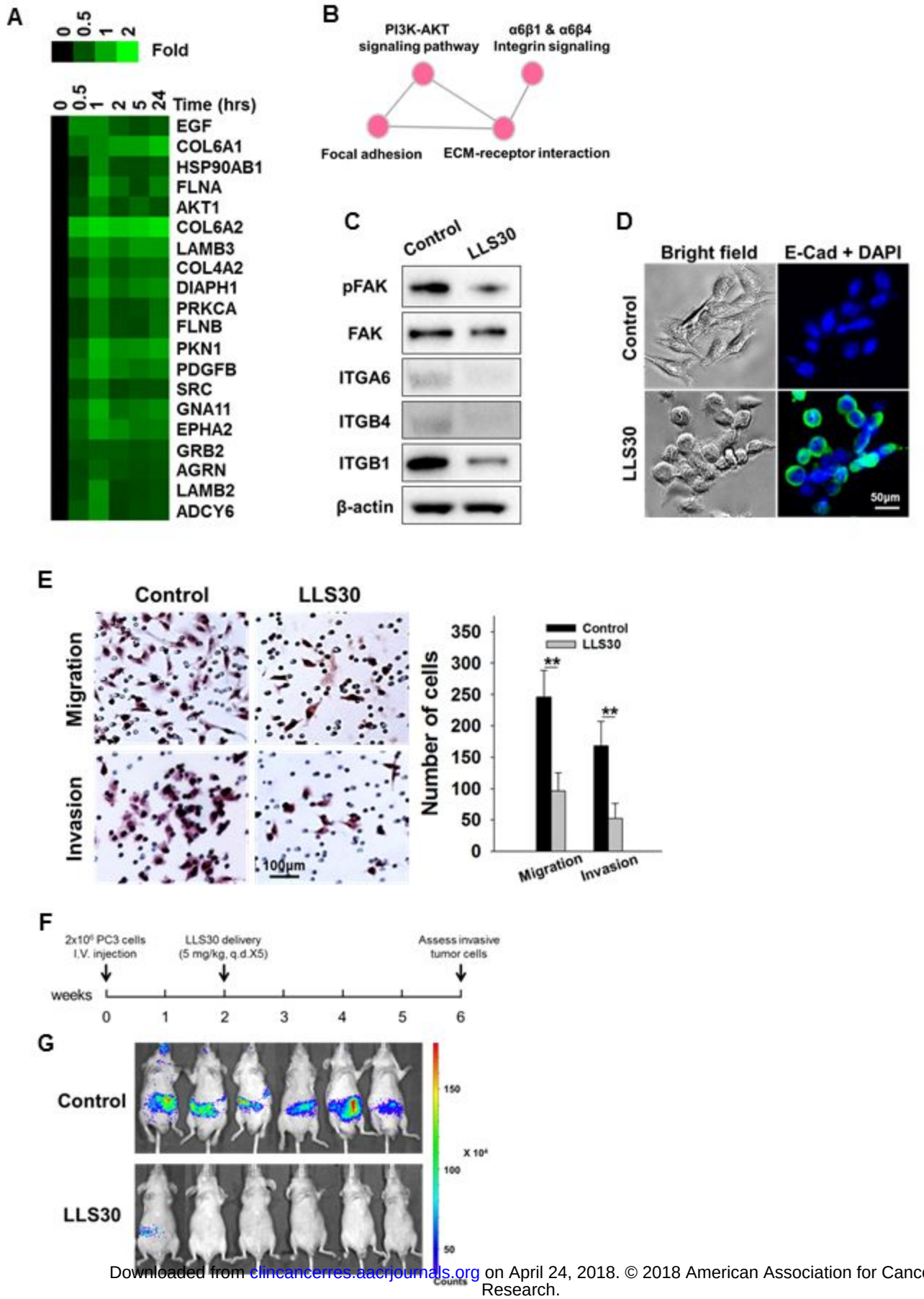

AACR American Association for Cancer Research

Clinical Cancer Research

Targeting Galectin-1 impairs castration-resistant prostate cancer progression and invasion

Tsung-Chieh Shih, Ruiwu Liu, Chun-Te Wu, et al.

Clin Cancer Res Published OnlineFirst April 17, 2018.